SUPPLEMENTARY INFORMATION

Computational Modeling Predicts the Stability of Both Pd^{+} and Pd^{2+} Ion-Exchanged into H-CHA

Jeroen Van der Mynsbrugge[a], Martin Head-Gordon[b] and Alexis T. Bell[a]*

[a]Department of Chemical and Biomolecular Engineering

University of California, Berkeley, CA 94720, USA

[b]Department of Chemistry

University of California, Berkeley, CA 94720, USA

Submitted to

Journal of Materials Chemistry A

(Date)

*To whom correspondence should be addressed: alexbell@berkeley.edu

1 Configurational search

Figure S1 illustrates the existence of various chemically equivalent but structurally different configurations for the H^+, Pd^0H^+ and Pd^+ species at isolated Al atoms, and for H^+/H^+, Pd^0 H^+/H^+, Pd^+/H^+ and Pd^{2+} species at the proximate Al pairs. For a given Al, three of its adjacent oxygen atoms are accessible from the CHA cage. The charge compensating H^+ (and therefore the coordinating Pd in Pd^0 H^+) can be located in three different positions. Similarly, Pd^+ can assume two different orientations, facing either the 6-ring or an adjacent 8-ring. While the configuration of Pd^{2+} is trivial, as it is expected to be located near the center of the 6-ring shared by the Al pair responsible for the counter charge, this is not the case for any of the other species. To identify the lowest-free energy structure for each of H^+, Pd^0H^+ and Pd^+ species at isolated Al atoms, and for H^+/H^+, Pd^0 H^+/H^+, Pd^+/H^+ and Pd^{2+} species at the proximate Al pairs in the 6-ring, we have examined all of the configurations that are schematically represented in Figure S1. Their relative free energies are shown in Table S1.

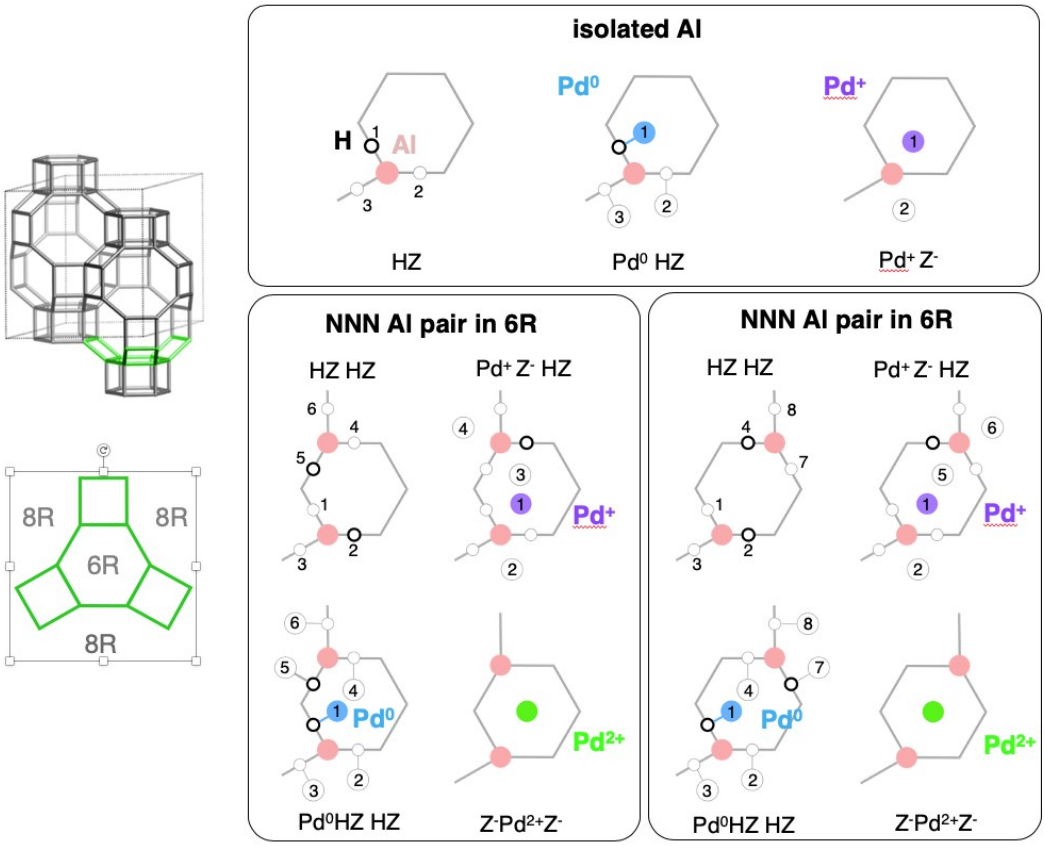

Figure S1. Schematic representation of the various chemically equivalent but structurally different configurations for Pd^{n+} (n=0,1,2) sites at isolated Al and proximate Al pairs in the 6-ring in CHA.

Table S1. Relative free energies (in kJ/mol) of the various chemically equivalent but structurally different configurations for Pd^{n+} (n=0,1,2) sites at isolated Al and proximate Al pairs in the 6-ring in CHA. LOT: ωB97X-D/def2-tzvpd // ωB97X-D/def2-sv(p); T=300 K, P=P_{atm}.

Isolated Al	
HZ	
h1	0
h2	+1
h3	+11
Pd^0 HZ	
h1-pd01	0
h2-pd02	+5
h3-pd03	+9
Pd^+Z^-	
pd11	0
pd12	+7
NNN Al pair	
HZ HZ	
h1-h4	+22
h1-h5	+35
h1-h6	+20
h2-h4	+44
h2-h5	0
h2-h6	+37
h3-h4	+40
h3-h5	+23
h3-h6	+49
Pd^0 HZ HZ	
h1-h4-pd01	+3
h1-h4-pd04	+3
h1-h5-pd01	0
h1-h5-pd05	+24
h1-h6-pd01	+8
h1-h6-pd06	+15
h2-h4-pd02	+37
h2-h4-pd04	+21
h2-h5-pd02	+4
h2-h5-pd05	+3
h2-h6-pd02	+34
h2-h6-pd06	+20

h3-h4-pd03	+34
h3-h4-pd04	+32
h3-h5-pd03	+8
h3-h5-pd05	+26
h3-h6-pd03	+41
h3-h6-pd06	+37
Pd^{+} Z^{-} HZ	
h1-pd13	+43
h1-pd14	+48
h2-pd13	+50
h2-pd14	+48
h3-pd13	+38
h3-pd14	+68
h4-pd11	+75
h4-pd12	+69
h5-pd11	0
h5-pd12	+36
h6-pd11	+39
h6-pd12	+73
NNNN Al pair	
HZ HZ	
h1-h4	+44
h1-h7	0
h1-h8	+20
h2-h4	0
h2-h7	+34
h2-h8	+26
h3-h4	+21
h3-h7	+26
h3-h8	+41
Pd^{0} HZ HZ	
h1-h4-pd01	+16
h1-h4-pd04	+15
h1-h7-pd01	0
h1-h7-pd07	+13
h1-h8-pd01	+20
h1-h8-pd08	+20
h2-h4-pd02	+13
h2-h4-pd04	+2
h2-h7-pd02	+39

h2-h7-pd07	+41
h2-h8-pd02	+38
h2-h8-pd08	+34
h3-h4-pd03	+20
h3-h4-pd04	+20
h3-h7-pd03	+35
h3-h7-pd07	+43
h3-h8-pd03	+45
h3-h8-pd08	+44
Pd^{+} Z^{-} HZ	
h1-pd15	+38
h1-pd16	+14
h2-pd15	0
h2-pd16	+37
h3-pd15	+4
h3-pd16	+42
h4-pd11	+37
h4-pd12	+15
h7-pd11	+1
h7-pd12	+36
h8-pd11	+4
h8-pd12	+42

2 Characteristic Pd-O distances for Pd^{2+}, $Pd^{+}H^{+}$ and $[Pd\text{-}O\text{-}Pd]^{2+}$

Table S2 compares the characteristic Pd-O distances in our model structures for Pd^{2+}, $Pd^{+}H^{+}$ and $[Pd\text{-}O\text{-}Pd]^{2+}$ at the NNNN Al pair in the 6-ring with those reported by Khivantsev et al. (ref. 17 in the main text) and Paolucci et al. (ref. 26 in the main text), showing excellent agreement despite the use of different computational methods.

Table S2. Comparison of the characteristic Pd-O distances in our model structures for Pd^{2+}, $Pd^{+}H^{+}$ and $[Pd\text{-}O\text{-}Pd]^{2+}$ at the NNNN Al pair in the 6-ring with those in similar structures reported by Khivantsev et al. (ref. 17 in the main text) and Paolucci et al. (ref. 26 in the main text).

	d(Pd-O_{zeo}) [Å]		
	This study	*Khivantsev et al.*[17]	*Paolucci et al.*[32]
Pd^{2+}	2.04; 2.04; 2.11; 2.11	2.06; 2.06; 2.14; 2.14	2.04; 2.04; 2.11; 2.11
Pd^{+}	2.23; 2.30; 2.33; 2.33	2.20; 2.22; 2.25	2.18–2.38
$[Pd\text{-}O\text{-}Pd]^{2+}$	2.10; 2.17; 2.11; 2.18	2.14; 2.19; 2.14; 2.19	

3 Validation of the QM region selections

To validate our choice of QM regions used to model Pd sites at the different proximate Al pairs in the 6-ring or 8-ring, additional test calculations were performed using the larger QM regions shown in Figure S2, which include the full 6-ring and 8-ring for all Al pairs. To ensure that the salient observations discussed in the main text are unaffected if only the ring in which both Al atoms are located is treated at the QM level, we have reoptimized the structures of $Pd^{+}H^{+}Z^{-}Z^{-}$ and $Pd^{2+}Z^{-}Z^{-}$ using the alternative QM regions and evaluated the effect of the QM region on the energies of formation of $Pd^{+}H^{+}Z^{-}Z^{-}$ and $Pd^{2+}Z^{-}Z^{-}$,which were ultimately found to be the most favorable species over a wide range of operating conditions for all Al pairs. The results of these calculations are shown in Figure S3 and Table S2.The same trends are obtained regardless of the QM region,

and crucially the *difference* in formation energy between $Pd^{+}H^{+}Z^{-}Z^{-}$ and $Pd^{2+}Z^{-}Z^{-}$ is reproduced within 12 kJ/mol or less (Table S2).

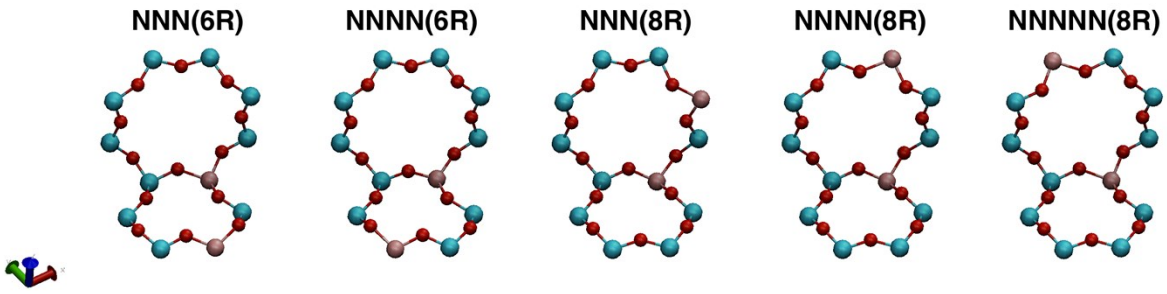

Figure S2. Alternative QM regions including both the 6-ring and the 8-ring for different proximate Al pairs in the 6-ring (NNN and NNNN) or 8-ring (NNN, NNNN and NNNNN). Si atoms are shown in cyan, Al in pink, O in red, H in white

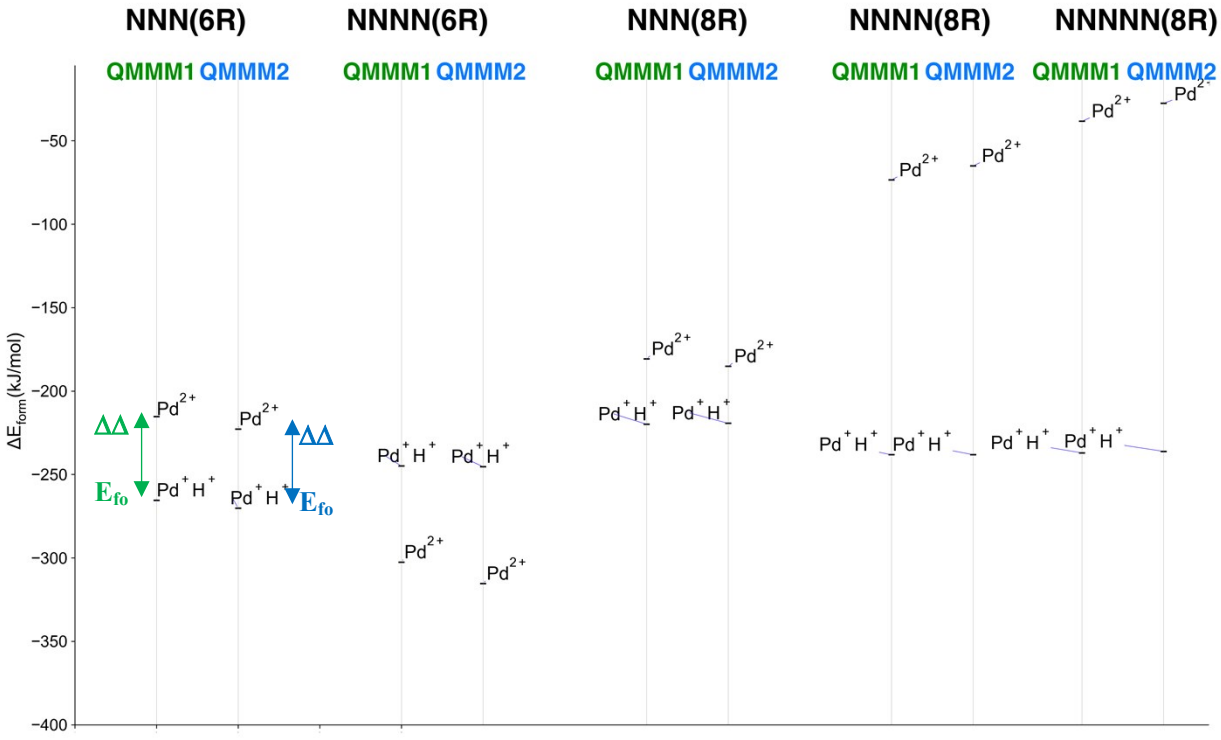

Figure S3. Formation energies of $Pd^{+}H^{+}Z^{-}Z^{-}$ and $Pd^{2+}Z^{-}Z^{-}$ at the different Al pairs in the 6-ring or 8-ring, evaluated at the ωB97X-D/def2-tzvpd // ωB97X-D/def2-sv(p) level of theory using the QM regions shown in Figure 1 in the main text (QMMM1) and using the alternative QM regions shown in Figure S2 (QMMM2).

Table S2. Differences in formation energies of $Pd^{+}H^{+}Z^{-}Z^{-}$ and $Pd^{2+}Z^{-}Z^{-}$ at the different Al pairs in the 6-ring or 8-ring, evaluated at the ωB97X-D/def2-tzvpd // ωB97X-D/def2-sv(p) level of theory using the QM regions shown in Figure 1 in the main text (QMMM1) and using the alternative QM regions shown in Figure S2 (QMMM2).

	$\Delta\Delta E_{form}(Pd^{+}H^{+}Z^{-}Z^{-} - Pd^{2+}Z^{-}Z^{-})$		
	QMMM1 kJ/mol	**QMMM2** kJ/mol	**|QMMM1 – QMMM2|** kJ/mol
NNN(6R)	-50	-47	3
NNNN(6R)	58	70	12
NNN(8R)	-39	-34	5
NNNN(8R)	-165	-173	8
NNNNN(8R)	-199	-209	10

4 Validation of the density functional selection

Additionally, we have evaluated the energies of formation of $Pd^{+}H^{+}Z^{-}Z^{-}$ and $Pd^{2+}Z^{-}Z^{-}$ using the wB97M-V functional to refine the energies of the structures of $Pd^{+}H^{+}Z^{-}Z^{-}$ and $Pd^{2+}Z^{-}Z^{-}$ obtained with the QM regions shown in Figure 1 in the main text to assess the effect of our choice of density functional. The results of these calculations are shown in Figure S4 and Table S3. Again, the same trends are obtained with either functional, and the difference in formation energy between $Pd^{+}H^{+}Z^{-}Z^{-}$ and $Pd^{2+}Z^{-}Z^{-}$ is reproduced within 9 kJ/mol or less (Table S3).

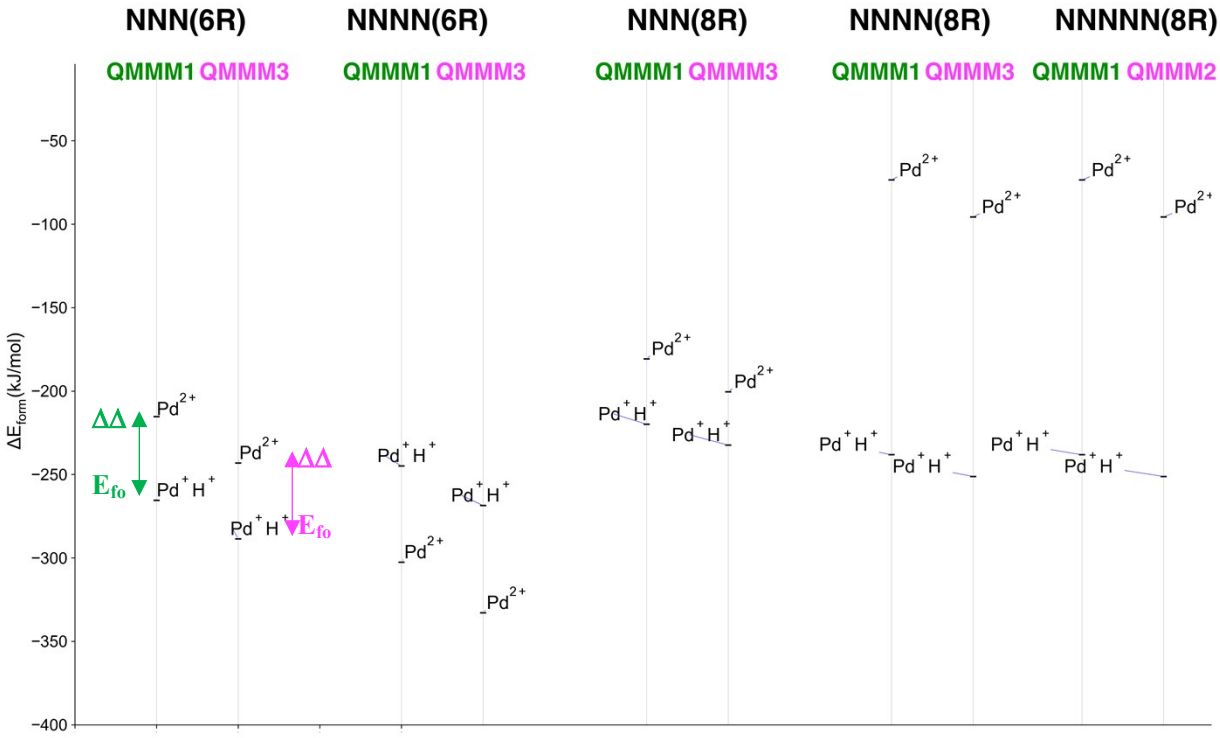

Figure S4. Formation energies of $Pd^{+}H^{+}Z^{-}Z^{-}$ and $Pd^{2+}Z^{-}Z^{-}$ at the different Al pairs in the 6-ring or 8-ring, evaluated using the QM regions shown in Figure 1 in the main text at the ωB97X-D/def2-tzvpd // ωB97X-D/def2-sv(p) level of theory (QMMM1) and at the ωB97M-V/def2-tzvpd // ωB97X-D/def2-sv(p) level of theory (QMMM3).

Table S3. Differences in formation energies of $Pd^{+}H^{+}Z^{-}Z^{-}$ and $Pd^{2+}Z^{-}Z^{-}$ at the different Al pairs in the 6-ring or 8-ring, evaluated using the QM regions shown in Figure 1 in the main text at the ωB97X-D/def2-tzvpd // ωB97X-D/def2-sv(p) level of theory (QMMM1) and at the ωB97M-V/def2-tzvpd // ωB97X-D/def2-sv(p) level of theory (QMMM3).

	$\Delta\Delta E_{form}(Pd^{+}H^{+}Z^{-}Z^{-} - Pd^{2+}Z^{-}Z^{-})$		
	QMMM1 kJ/mol	**QMMM3** kJ/mol	|**QMMM1** – **QMMM3**| kJ/mol
NNN(6R)	-50	-46	4
NNNN(6R)	58	64	7
NNN(8R)	-39	-32	7
NNNN(8R)	-165	-156	9
NNNNN(8R)	-199	-193	6

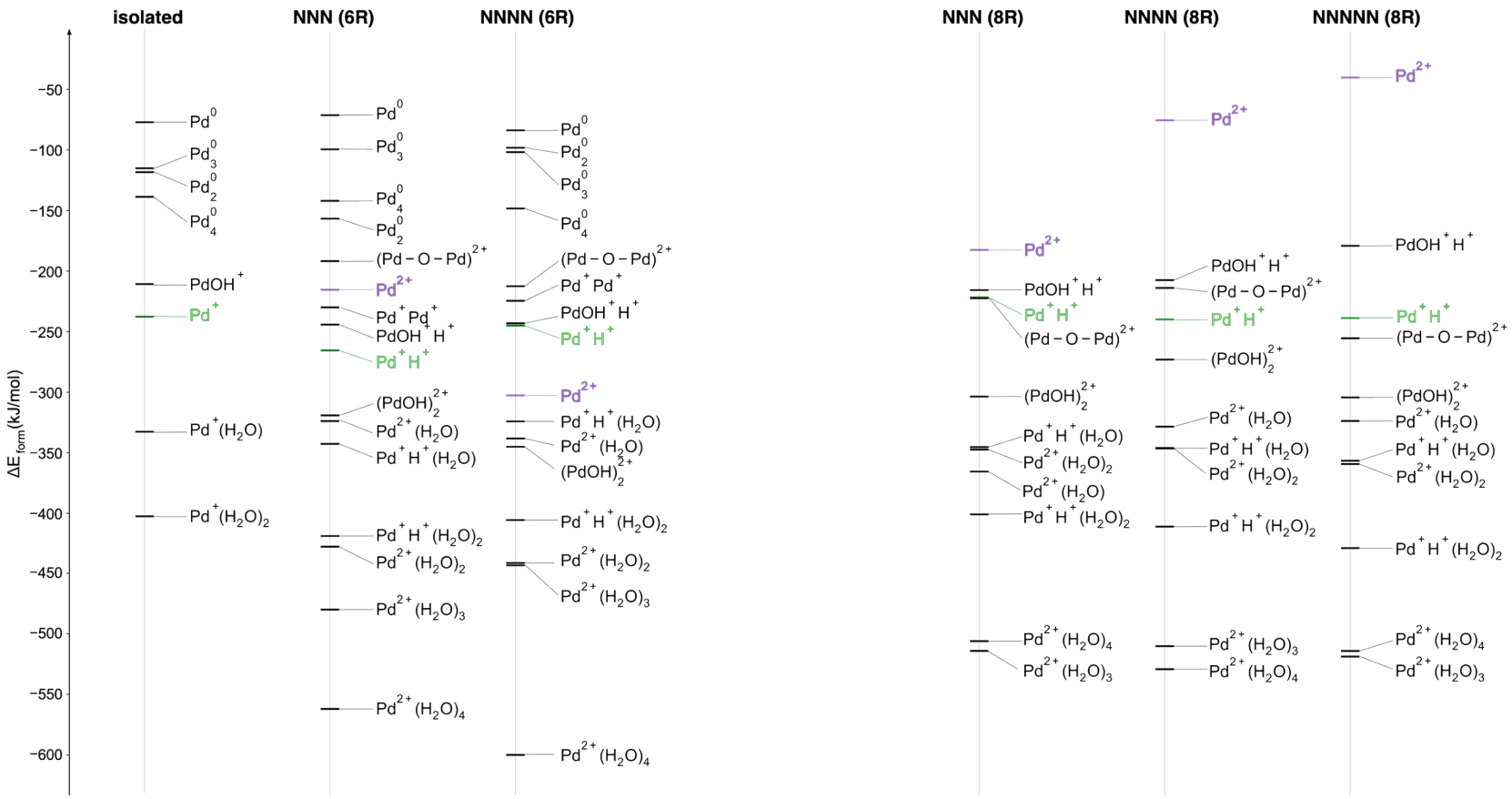

Figure S5. Electronic energies of formation (ΔE_{form}) for the Pd species in both the 6-ring (ΔG_{form} in Figure 4 of main text) and in the 8-ring (ΔG_{form} in Figure 8 of main text).

5 Phase diagrams

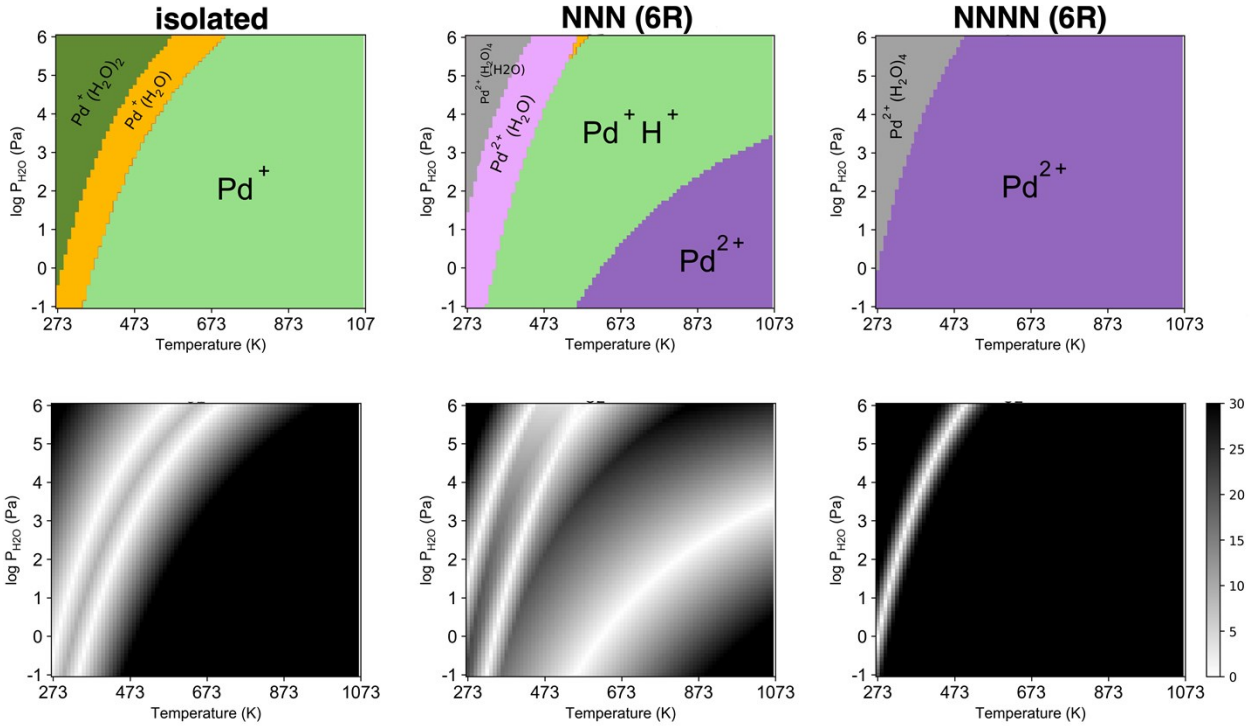

Figure S6. [P_{H2O},T] phase diagrams showing the thermodynamically preferred Pd species (top row; Figure 5 in the main text) and corresponding heat maps (bottom row) illustrating the difference in free energy of formation (in kJ/mol) between the thermodynamically preferred Pd species and the species with the next-lowest free energy at isolated Al and Al pairs – next-next-nearest neighbors (NNNN) and next-nearest neighbors (NNN) – in the 6-ring of H-CHA under flowing air (p_{O2} = 20 kPa).

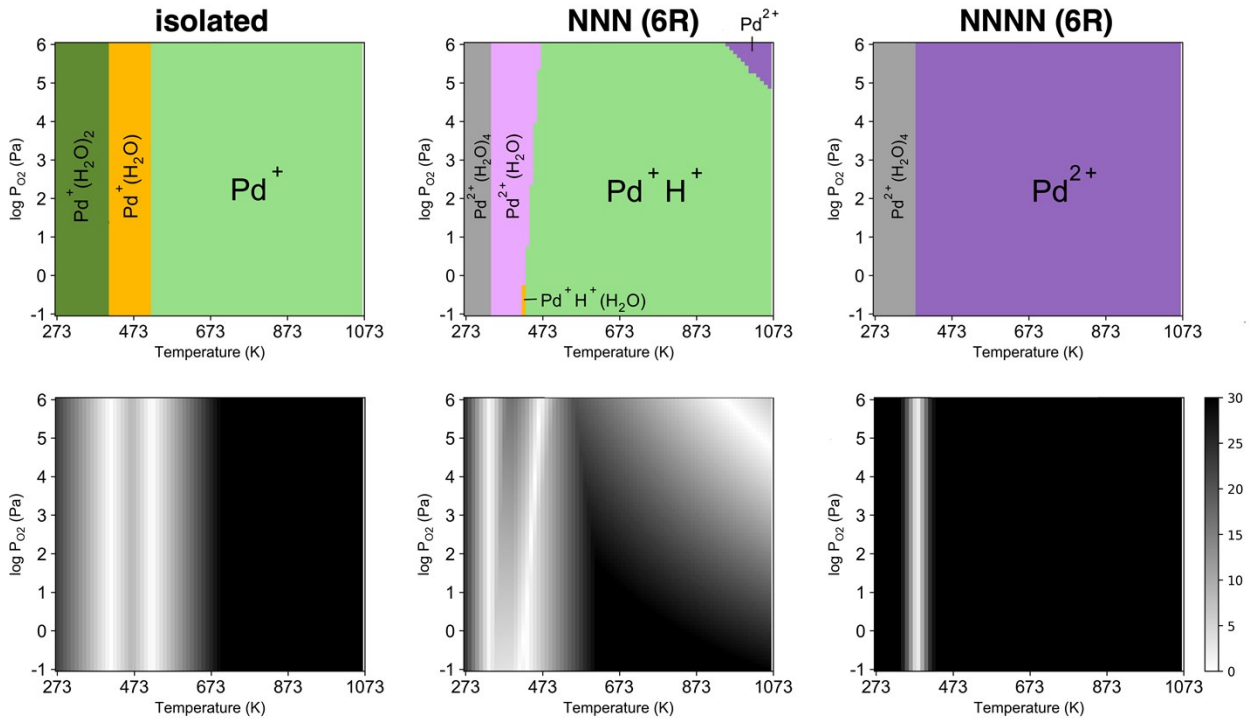

Figure S7. [P_{O2},T] phase diagrams showing the thermodynamically preferred Pd species (top row) and corresponding heat maps (bottom row) illustrating the difference in free energy of formation (in kJ/mol) between the thermodynamically preferred Pd species and the species with the next-lowest free energy at isolated Al and Al pairs – next-next-nearest neighbors (NNNN) and next-nearest neighbors (NNN) – in the 6-ring of H-CHA under oxidizing conditions with 5% water (p_{H2O} = 5 kPa).

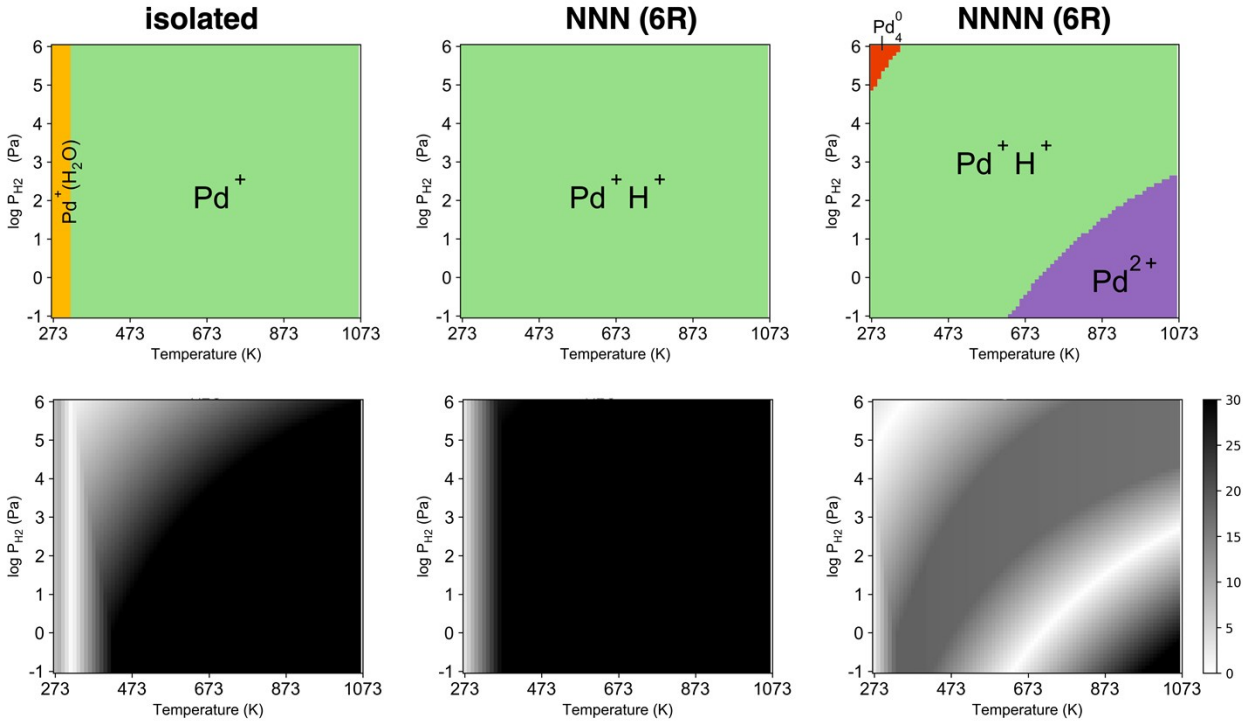

Figure S8. [P_{H2},T] phase diagrams showing the thermodynamically preferred Pd species (top row; Figure 7 in the main text) and corresponding heat maps (bottom row) illustrating the difference in free energy of formation (in kJ/mol) between the thermodynamically preferred Pd species and the species with the next-lowest free energy at isolated Al and Al pairs – next-next-nearest neighbors (NNNN) and next-nearest neighbors (NNN) – in the 6-ring of H-CHA under dry reducing conditions (p_{H2O} = 0.01 Pa).

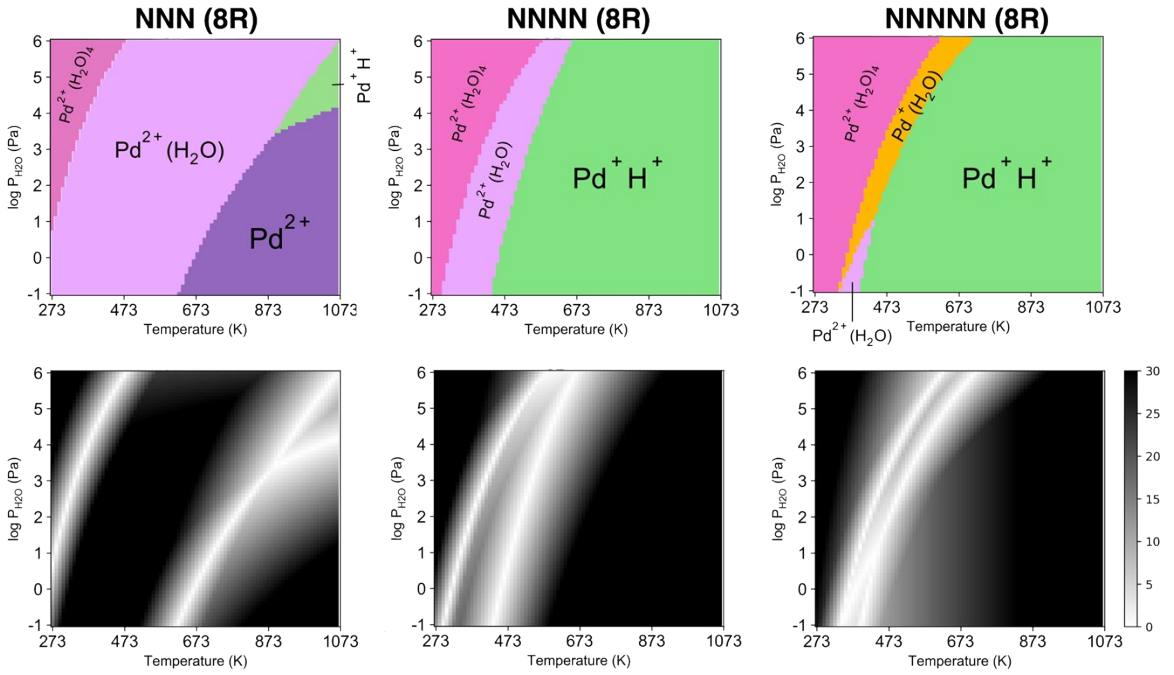

Figure S9. [P_{H2O},T] phase diagrams showing the thermodynamically preferred Pd species (top row; Figure 9 in the main text) and corresponding heat maps (bottom row) illustrating the difference in free energy of formation (in kJ/mol) between the thermodynamically preferred Pd species and the species with the next-lowest free energy at next-nearest neighbors (NNN), next-next-nearest neighbors (NNNN), next-next-next-nearest neighbors (NNNNN) Al pairs in the 8-ring of H-CHA under flowing air (p_{O2} = 20 kPa).

6 Alternative 3D representations of select structures

Because of the nature of the CHA (a dense 3D network of interconnected cages) it is difficult to show the active sites in their framework context in a single 2D representation without confusing the reader. For this reason, we have opted to omit the MM atoms in the Figures included in the manuscript. Below are a few additional figures showing an alternative representation for a selection of structures. The QM atoms are shown in ball-and-stick representation; the remaining atoms of the central *cha* cage are shown as a bolder wireframe for visual clarity (as in Figure 1 in the main text).

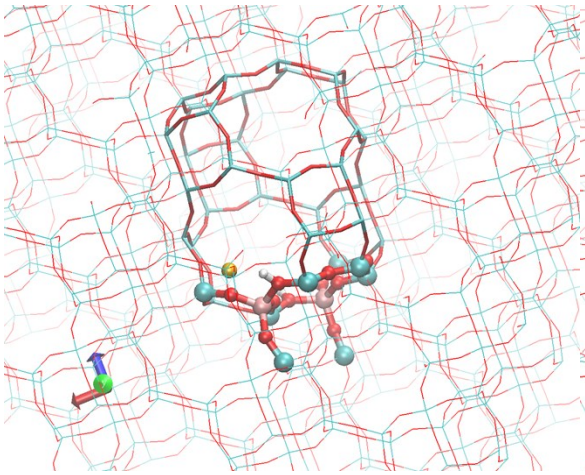

HZ Pd^0 HZ NNN(6R)

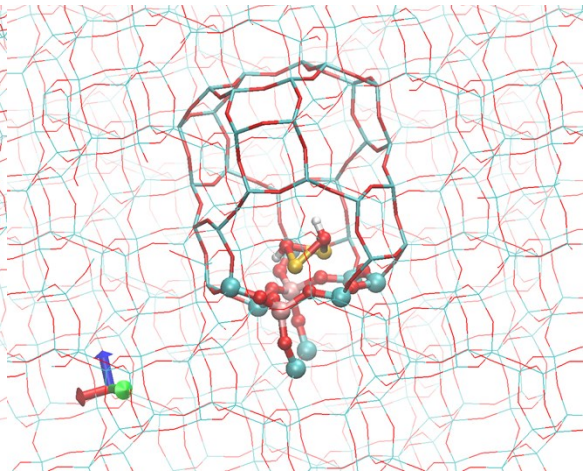

Z^- $(PdOH)_2^{2+}$ Z^- NNN(6R)

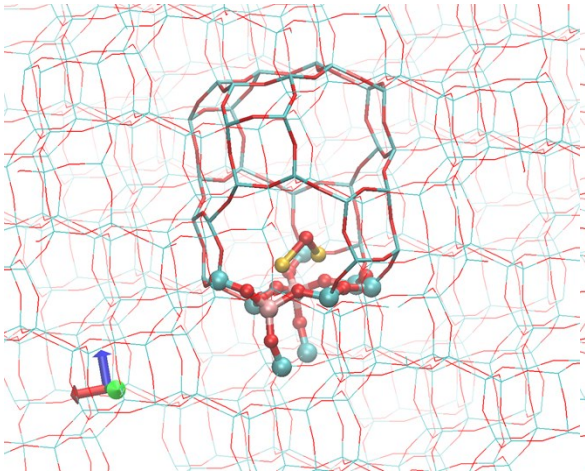

Z^- $(Pd\text{-}O\text{-}Pd)^{2+}$ Z^- NNN(6R)

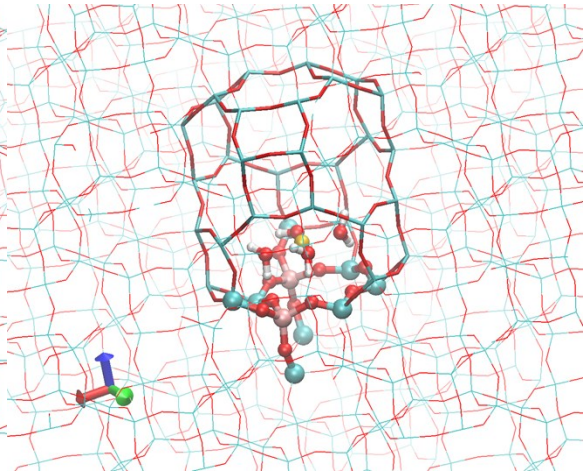

Z^- $Pd^{2+}(H_2O)_4$ Z^- NNN(6R)

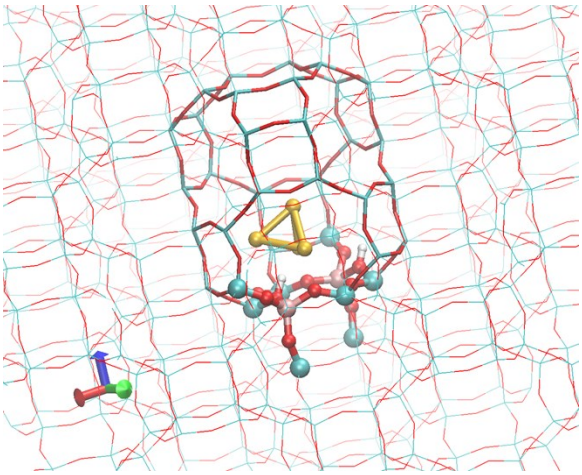

HZ Pd_4^0 HZ NNNN(6R)

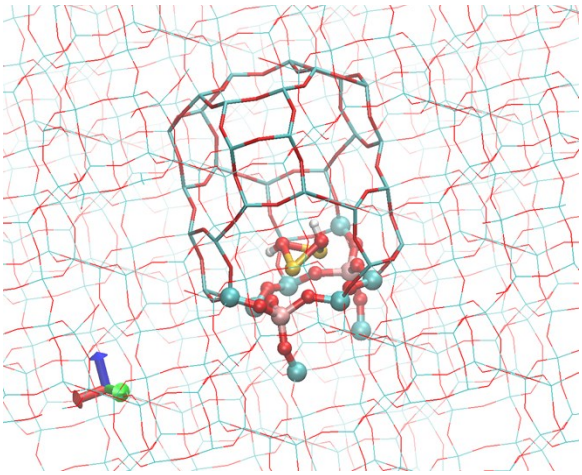

Z^- $(PdOH)_2^{2+}$ Z^- NNNN(6R)

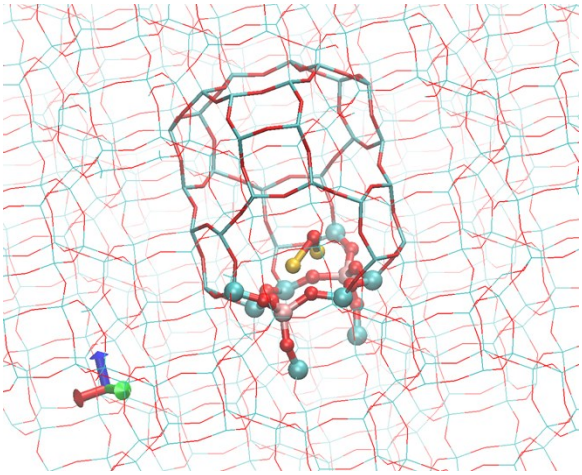

Z^- $(Pd\text{-}O\text{-}Pd)^{2+}$ Z^- NNN(6R)

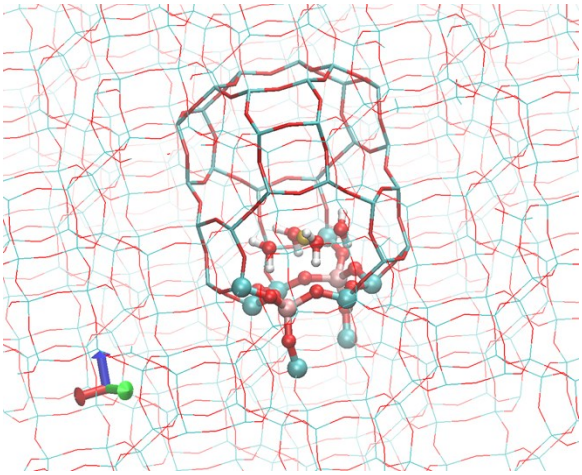

Z^- $Pd^{2+}(H_2O)_4$ Z^- NNN(6R)

7 XYZ coordinates of all stationary points

See ZIP archive; QM atoms are grouped at the top of each geometry.

Description	Filename	# QM atoms
isolated Al		
HZ	001.xyz	17
Pd^0 HZ	002.xyz	18
Pd_2^0 HZ	003.xyz	19
Pd_3^0 HZ	004.xyz	20
Pd_4^0 HZ	005.xyz	21
Pd^+ Z^-	006.xyz	17
$Pd^+(H_2O)$ Z^-	007.xyz	20
$Pd^+(H_2O)_2$ Z^-	008.xyz	23
$PdOH^+$ Z^-	009.xyz	19
NNN(6R)		
HZ HZ	010.xyz	22
HZ Pd^0 HZ	011.xyz	23
HZPd_2^0 HZ (Z⁻ Pd_2H^+ HZ)	012.xyz	24
HZ Pd_3^0 HZ	013.xyz	25
HZ Pd_4^0 HZ	014.xyz	26
HZ Pd^+ Z^-	015.xyz	22
HZ $Pd^+(H_2O)$ Z^-	016.xyz	25
HZ $Pd^+(H_2O)_2$ Z^-	017.xyz	28
Z^-Pd^+ Pd^+Z^-	018.xyz	22
Z^- Pd^{2+} Z^-	019.xyz	21
Z^- $Pd^{2+}(H_2O)$ Z^-	020.xyz	24
Z^- $Pd^{2+}(H_2O)_2$ Z^-	021.xyz	27
Z^- $Pd^{2+}(H_2O)_3$ Z^-	022.xyz	30
Z^- $Pd^{2+}(H_2O)_4$ Z^-	023.xyz	33
HZ $PdOH^+$ Z^-	024.xyz	24
Z^- $(PdOH)_2^{2+}$ Z^-	025.xyz	26
Z^- $(Pd\text{-}O\text{-}Pd)^{2+}$ Z^-	026.xyz	23
NNNN(6R)		
HZ HZ	027.xyz	22
HZ Pd^0 HZ	028.xyz	23
HZPd_2^0 HZ	029.xyz	24
HZ Pd_3^0 HZ	030.xyz	25
HZ Pd_4^0 HZ	031.xyz	26
HZ Pd^+ Z^-	032.xyz	22
HZ $Pd^+(H_2O)$ Z^-	033.xyz	25
HZ $Pd^+(H_2O)_2$ Z^-	034.xyz	28

$Z^{-}Pd^{+}$ $Pd^{+}Z^{-}$	035.xyz	22
Z^{-} Pd^{2+} Z^{-}	036.xyz	21
Z^{-} $Pd^{2+}(H_2O)$ Z^{-}	037.xyz	24
Z^{-} $Pd^{2+}(H_2O)_2$ Z^{-}	038.xyz	27
Z^{-} $Pd^{2+}(H_2O)_3$ Z^{-}	039.xyz	30
Z^{-} $Pd^{2+}(H_2O)_4$ Z^{-}	040.xyz	33
HZ $PdOH^{+}$ Z^{-}	041.xyz	24
Z^{-} $(PdOH)_2^{2+}$ Z^{-}	042.xyz	26
Z^{-} $(Pd\text{-}O\text{-}Pd)^{2+}$ Z^{-}	043.xyz	23
NNN(8R)		
HZ HZ	044.xyz	26
HZ Pd^{+} Z^{-}	045.xyz	26
HZ $Pd^{+}(H_2O)$ Z^{-}	046.xyz	29
HZ $Pd^{+}(H_2O)_2$ Z^{-}	047.xyz	32
Z^{-} Pd^{2+} Z^{-}	048.xyz	25
Z^{-} $Pd^{2+}(H_2O)$ Z^{-}	049.xyz	28
Z^{-} $Pd^{2+}(H_2O)_2$ Z^{-}	050.xyz	31
Z^{-} $Pd^{2+}(H_2O)_3$ Z^{-}	051.xyz	34
Z^{-} $Pd^{2+}(H_2O)_4$ Z^{-}	052.xyz	37
HZ $PdOH^{+}$ Z^{-}	053.xyz	28
Z^{-} $(PdOH)_2^{2+}$ Z^{-}	054.xyz	30
Z^{-} $(Pd\text{-}O\text{-}Pd)^{2+}$ Z^{-}	055.xyz	27
NNNN(8R)		
HZ HZ	056.xyz	26
HZ Pd^{+} Z^{-}	057.xyz	26
HZ $Pd^{+}(H_2O)$ Z^{-}	058.xyz	29
HZ $Pd^{+}(H_2O)_2$ Z^{-}	059.xyz	32
Z^{-} Pd^{2+} Z^{-}	060.xyz	25
Z^{-} $Pd^{2+}(H_2O)$ Z^{-}	061.xyz	28
Z^{-} $Pd^{2+}(H_2O)_2$ Z^{-}	062.xyz	31
Z^{-} $Pd^{2+}(H_2O)_3$ Z^{-}	063.xyz	34
Z^{-} $Pd^{2+}(H_2O)_4$ Z^{-}	064.xyz	37
HZ $PdOH^{+}$ Z^{-}	065.xyz	28
Z^{-} $(PdOH)_2^{2+}$ Z^{-}	066.xyz	30
Z^{-} $(Pd\text{-}O\text{-}Pd)^{2+}$ Z^{-}	067.xyz	27
NNNNN(8R)		
HZ HZ	068.xyz	26
HZ Pd^{+} Z^{-}	069.xyz	26
HZ $Pd^{+}(H_2O)$ Z^{-}	070.xyz	29
HZ $Pd^{+}(H_2O)_2$ Z^{-}	071.xyz	32
Z^{-} Pd^{2+} Z^{-}	072.xyz	25
Z^{-} $Pd^{2+}(H_2O)$ Z^{-}	073.xyz	28

$Z^- Pd^{2+}(H_2O)_2\ Z^-$	074.xyz	31
$Z^- Pd^{2+}(H_2O)_3\ Z^-$	075.xyz	34
$Z^- Pd^{2+}(H_2O)_4\ Z^-$	076.xyz	37
$HZ\ PdOH^+\ Z^-$	077.xyz	28
$Z^-\ (PdOH)_2^{2+}\ Z^-$	078.xyz	30
$Z^-\ (Pd\text{-}O\text{-}Pd)^{2+}\ Z^-$	079.xyz	27